Supplementary Information for

Bridging Crystalline MOFs with Atomically Dispersed Metal–Nitrogen–Carbon Catalysts via Structure Encoding

Daichi Homma,[a] Po-Wen Chung,[bcd] Shin R. Mukai,[e] Isao Ogino[e]*

[a]Graduate School of Chemical Sciences and Engineering, Hokkaido University, Sapporo, Hokkaido 060-8628, Japan

[b]Institute of Chemistry, Academia Sinica, Taipei 11529, Taiwan

[c]Department of Chemistry, National Taiwan University, Taipei 10617, Taiwan

[d]Department of Chemistry, National Sun Yat-sen University, Kaohsiung 80424, Taiwan

[e]Faculty of Engineering, Hokkaido University, Sapporo, Hokkaido 060-8628, Japan

E-mail: iogino@eng.hokudai.ac.jp

Table of contents

S1. Materials and methods

S1-1. Chemicals and materials

Zinc nitrate hexahydrate (99.0%, Kanto Chemical), zinc acetate dihydrate (99.0%, Fujifilm Wako), zinc oxide (99.0%, Fujifilm Wako), imidazole (Im, 98.0%, Fujifilm Wako), 2-methylimidazole (2-mIm, 98.0%, TCI), 2-ethylimidazole (2-eIm, 98.0%, TCI), benzimidazole (bIm, 98.0%, TCI), 5-chlorobenzimidazole (5-cbIm, 98.0%, TCI), 4,5-dichloroimidazole (4,5-dcIm, 97.0%, TCI), methanol (99.8%, Fujifilm Wako), *N,N*-dimethylformamide (DMF, 99.5%, Fujifilm Wako), 1-propanol (99.5%, Fujifilm Wako), 2-propanol (99.7%, Fujifilm Wako), chloroform (99.0%, Fujifilm Wako), cyclohexane (98.0%, Fujifilm Wako), toluene (99.5%, Fujifilm Wako), 25% ammonia solution (Wako 1st Grade, Fujifilm Wako), and iron(III) chloride hexahydrate (99.0%, Fujifilm Wako) were used.

S1-2. Synthesis of precursor MOFs

ZIF-4, ZIF-7, ZIF-8, ZIF-11, ZIF-71, ZIF-95 and MAF-6 were synthesized according to the method reported procedures with slight modifications.

ZIF-4:[1] A solid mixture of $Zn(NO_3)_2 \cdot 6H_2O$ (1.820 g, 6.12 mmol) and Im 1.200 g, 17.6 mmol) was dissolved in 120 mL DMF in a Teflon-lined stainless-steel autoclave (Parr Instrument Company, Model 4744). This was capped and heated at 100 ºC for 48 h in a programmable oven (Plus Ko-lab, Korea), then cooled to room temperature. Colorless crystals of ZIF-4 thus produced were washed with DMF (100 mL) and methanol (100 mL) and dried in the air (2 h) (yield:17% based on zinc nitrate hexahydrate).

ZIF-7:[2] A solid mixture of $Zn(NO_3)_2 \cdot 6H_2O$ (0.508 g, 1.71 mmol) and bIm (1.292 g, 10.9 mmol) was dissolved in 168 mL DMF at room temperature. The synthesis was carried out at 50 °C for 46 h. The synthesis mixture was centrifuged for 15 minutes at 8000 rpm to recover ZIF-7 which was then washed with 80 mL methanol three times. The crystals were then dried in the air overnight (yield: 49% based on zinc nitrate hexahydrate).

ZIF-8:[3] $Zn(NO_3)_2 \cdot 6H_2O$ (8.27 g, 27.8 mmol) was dissolved in 400 mL methanol. To this, a solution of 2-mIm (9.23 g, 112 mmol) in 400 mL methanol was added. The reaction mixture was stirred at 800 rpm for 18 h at room temperature. The synthesis mixture was centrifuged for 15 minutes at 9000 rpm to recover ZIF-8 which was then washed with 160 mL methanol three times. The crystals were then dried in the air overnight (yield: 33% based on zinc nitrate hexahydrate).

ZIF-11:[4] Benzimidazole (0.96 g, 8.1 mmol) was dissolved in 15 mL methanol, 21 mL toluene and 0.5 mL ammonium hydroxide solution (25%). To this, a solution of $Zn(OAc)_2 \cdot 2H_2O$ (0.44 g, 2 mmol) in 10 mL methanol was added. The reaction mixture was stirred at 400 rpm for 2 h at room temperature. The ZIF-11 crystals were recovered by vacuum filtration, washed with methanol, and dried in the air overnight (yield: 88% based on zinc nitrate hexahydrate).

ZIF-71:[5] A solution of $Zn(OAc)_2 \cdot 2H_2O$ (0.351 g, 1.60 mmol) in 180 mL of 1-propanol and a solution of 4,5-dcIm (0.877 g, 6.40 mmol) in 60 mL of 1-propanol, were combined in a sealed vial and let stand at room temperature for 24 h. The 1-propanol was then removed from the vial using a pipette and the remaining crystals were soaked in chloroform (2 × 60 mL) for three days. To recover the crystals, the solution was centrifuged for 10 minutes at 9000 rpm and the chloroform was decanted. The crystals were then dried in the air (yield: 92% based on zinc acetate).

ZIF-95:[6] A solid mixture of $Zn(NO_3)_2 \cdot 6H_2O$ (0.125 g, 0.42 mmol) and 4,5-cbIm (0.733 g, 4.40 mmol) was dissolved in 33 mL DMF and 3 mL H_2O in a Teflon-lined stainless steel autoclave sealed tightly and heated at 120 °C for 72 h to give light yellow plate crystals. The reaction mixture was allowed to cool gradually to room temperature and crystals were washed with 50 mL DMF and then washed with 100 mL methanol. The solid ZIF-95 was dried in the air (yield: 66% based on zinc nitrate hexahydrate).

MAF-6:[7] ZnO (0.326 g, 4.00 mmol) was dissolved in 60 mL ammonium hydroxide solution (25%). To this, a solution of 2-eIm (0.769 g, 7.96 mmol) in 57 mL methanol and 3mL cyclohexane was added. The reaction mixture was stirred vigorously for 20 min at room temperature. The MAF-6 crystals were recovered by vacuum filtration, washed with 300 mL methanol, and dried in the air overnight (yield: 39% based on zinc oxide).

S1-3. Field emission scanning electron microscopy (FE-SEM)

Morphology of the samples was characterized by FE-SEM (JSM-7200F JEOL Ltd). Each sample was fixed to a sample stand using carbon tape. Acceleration voltages of 10.0 kV or 15.0 kV were used.

.

S2. Structural parameters of MOFs

Table S1. Crystallographic topology and structural parameters of the parent MOF frameworks used in this study. Reported parameters include framework topology, largest ring size (n), diameter of the largest included sphere (D_i), diameter of the largest free sphere (D_f), cavity-to-window size ratio (D_i/D_f), metal atom density (T/V), linker-liner distance (d_{L-L}), and linker N/C ratio.

Common name	Composition	topology	n^a	D_i /Å	D_f /Å	D_i / D_f	T / V /nm^{-3}	d_{L-L} /Å	Linker N/C ratio
ZIF-4	$Zn(Im)_2$	cag	6	4.74	2.41	1.97	3.68	1.21	0.67
ZIF-7	$Zn(bIm)_2$	sod	6	5.59	2.40	2.33	2.50	1.20	0.29
ZIF-8	$Zn(mIm)_2$	sod	6	11.39	3.41	3.34	2.45	1.71	0.50
ZIF-11	$Zn(bIm)_2$	rho	8	14.86	2.46	6.04	2.02	0.94	0.29
ZIF-71	$Zn(dcIm)_2$	rho	8	17.02	5.46	3.12	2.06	2.09	0.67
ZIF-95	$Zn(cbIm)_2$	poz	12	21.10	4.63	4.56	1.51	1.20	0.29
MAF-6	$Zn(eIm)_2$	rho	8	18.78	7.32	2.57	1.91	2.80	0.40

S3. X-ray photoelectron spectroscopy of MOF-derived carbons

Table S2. Elemental compositions and nitrogen speciation of MOF-derived carbons as determined by XPS.

	C / atomic%	N / atomic%				O / atomic%	Zn / atomic%
		pyridinic	pyrrolic	graphitic	total		
ZIF4-C	83.56	1.43	1.19	0.94	3.56	11.75	1.12
ZIF7-C	87.81	0.92	0.55	1.05	2.52	9.41	0.25
ZIF8-C	90.27	1.56	0.43	1.28	3.27	5.86	0.60
ZIF11-C	88.06	0.88	0.31	1.09	2.28	9.30	0.35
ZIF71-C	86.84	1.41	0.90	1.32	3.63	9.16	0.37
ZIF95-C	88.35	1.42	0.47	1.47	3.35	8.04	0.26
MAF6-C	90.72	1.52	0.42	1.51	3.45	5.05	0.77

S4. Bulk Fe content analyzed by ICP-OES and calculated Fe utilization

Table S3. Bulk Fe content of selected Fe–N–C catalysts determined by ICP-OES, Fe–N_x SD, and Fe utilization defined as the fraction of bulk Fe atoms present as Fe–N_x sites.

	Fe content/wt%	Fe–N_x SD/10^{18} sites g^{-1}	Fe utilization/atomic %[a]
Fe-ZIF7-C	0.7	2.9	3.8
Fe-ZIF8-C	1.9	8.7	4.3
Fe-MAF6-C	1.7	9.7	5.3

[a]Fe utilization (atomic %) = (SD × MW_{Fe})/($Fe_{wt\%}$/100×N_A), where SD is the Fe–N_x site density (sites g^{-1}), MW_{Fe} = 55.85 g mol^{-1}, $Fe_{wt\%}$ is the bulk Fe content from ICP-OES, and N_A is Avogadro's number.

S5. Comparison of Fe–N_x active site density and nitrogen coordination sites

Table S4. Fe–N_x site density and relative abundance of nitrogen coordination sites.

	Fe-N_x site density /10^{18} sites g^{-1}	N_4 sites/(Fe–N_x site density) ratio[a]
Fe-ZIF7-C	2.9	61
Fe-ZIF8-C	8.7	28
Fe-MAF6-C	9.7	24

[a]The number of N_4 sites was estimated by summing the total pyridinic and pyrrolic nitrogen contents determined by XPS and dividing the total by 4.

S6. Promising precursor MOF candidates

Table S5. MOFs with large d_{L-L} values identified as promising precursors for Fe–N–C catalysts. The structures were screened from a literature under the criteria that the metal cation is Zn^{2+} and the liners are limited to imidazolate derivatives. For ZIF-70, the MOF-C micropore volume (V_{micro}) shown in parentheses was estimated by extrapolating the regression line shown in Figure 2(d).

ID	Composition[a]	topology	D_f / Å	MR[b]	d_{L-L} / Å	MOF-C V_{micro} / $cm^3\ g^{-1}$
ZIF-70	$Zn(Im)_{1.13}(nIm)_{0.87}$	gme	13.38	12	3.46	(0.62)
ZIF-60	$Zn_2(Im)_3(mIm)$	mer	7.61	8	2.91	-
ZIF-10	$Zn(Im)_2$	mer	7.49	8	2.87	-
ZIF-725	$Zn(brbIm)_{1.35}(nIm)_{0.4}(Im)_{0.25}$	bam	21.69	24	2.83	-
MAF-6	$Zn(eIm)_2$	rho	7.32	8	2.80	0.53
ZIF-8	$Zn(mIm)_2$	sod	3.41	6	1.71	0.38

[a]Im: imidazolate, nIm: 2-methylimidazolate, brbIm: 5-bromobenzimidazolate.

[b]Ring size consisting of the largest pore aperture.

S7. Powder X-ray diffraction of synthesized MOFs

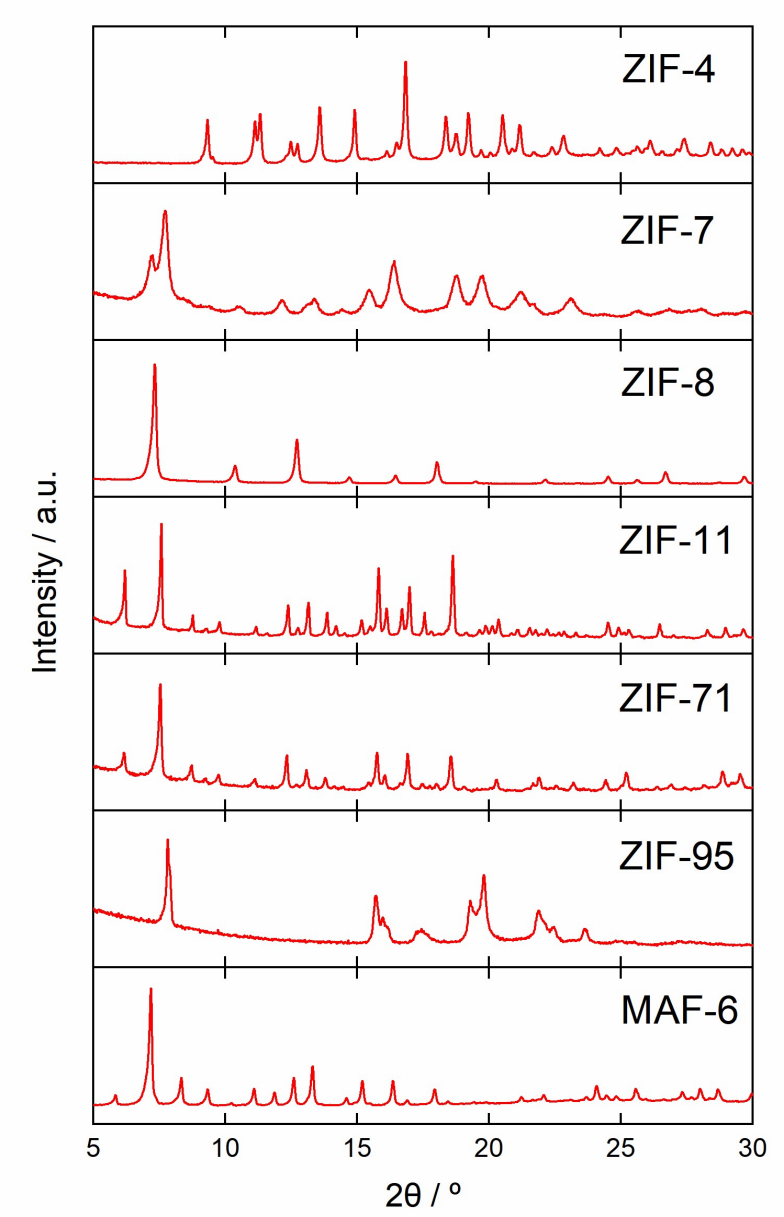

Figure S1. Powder X-ray diffraction patterns characterizing synthesized MOFs.

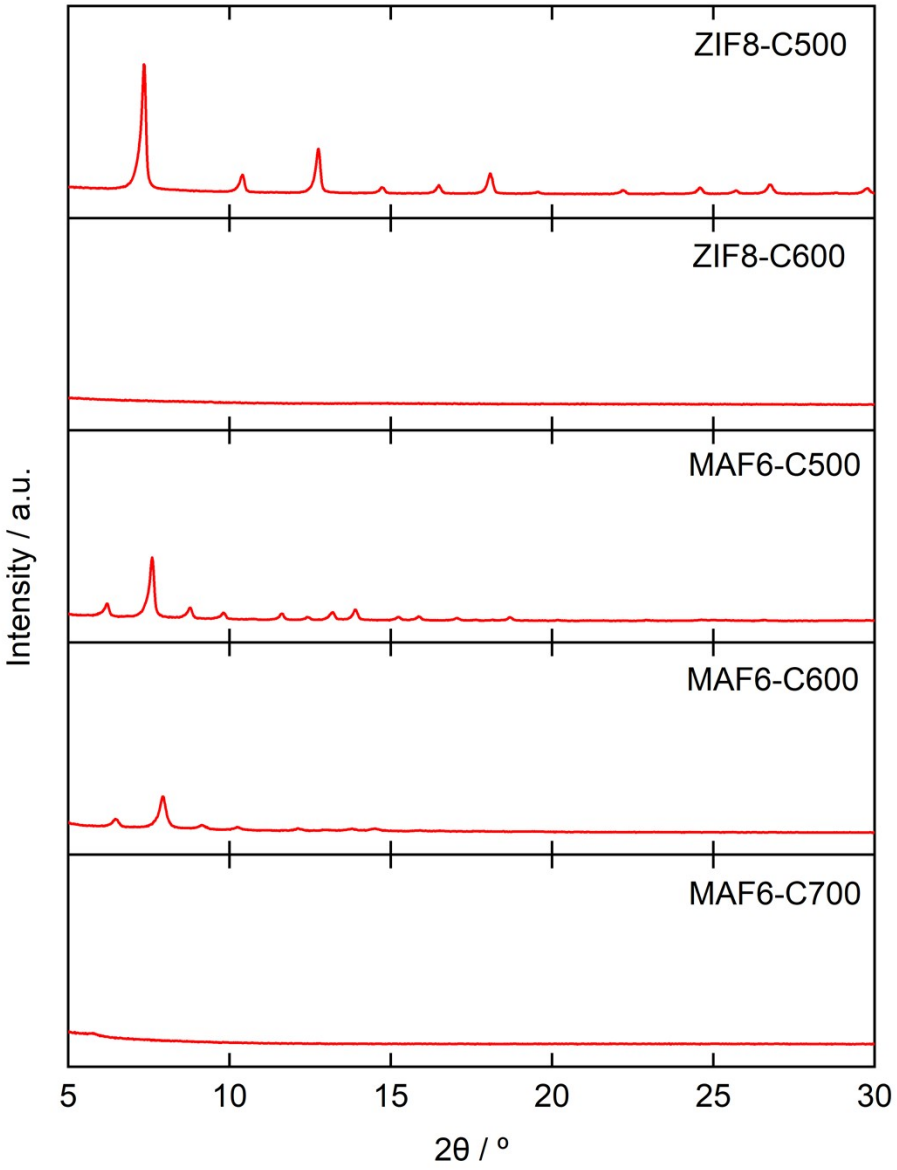

Figure S2. Powder X-ray diffraction patterns characterizing ZIF-8 and MAF-6 pyrolyzed at 500, 600 and 700 °C.

S8. FE-SEM characterization of synthesized MOFs and carbonized samples

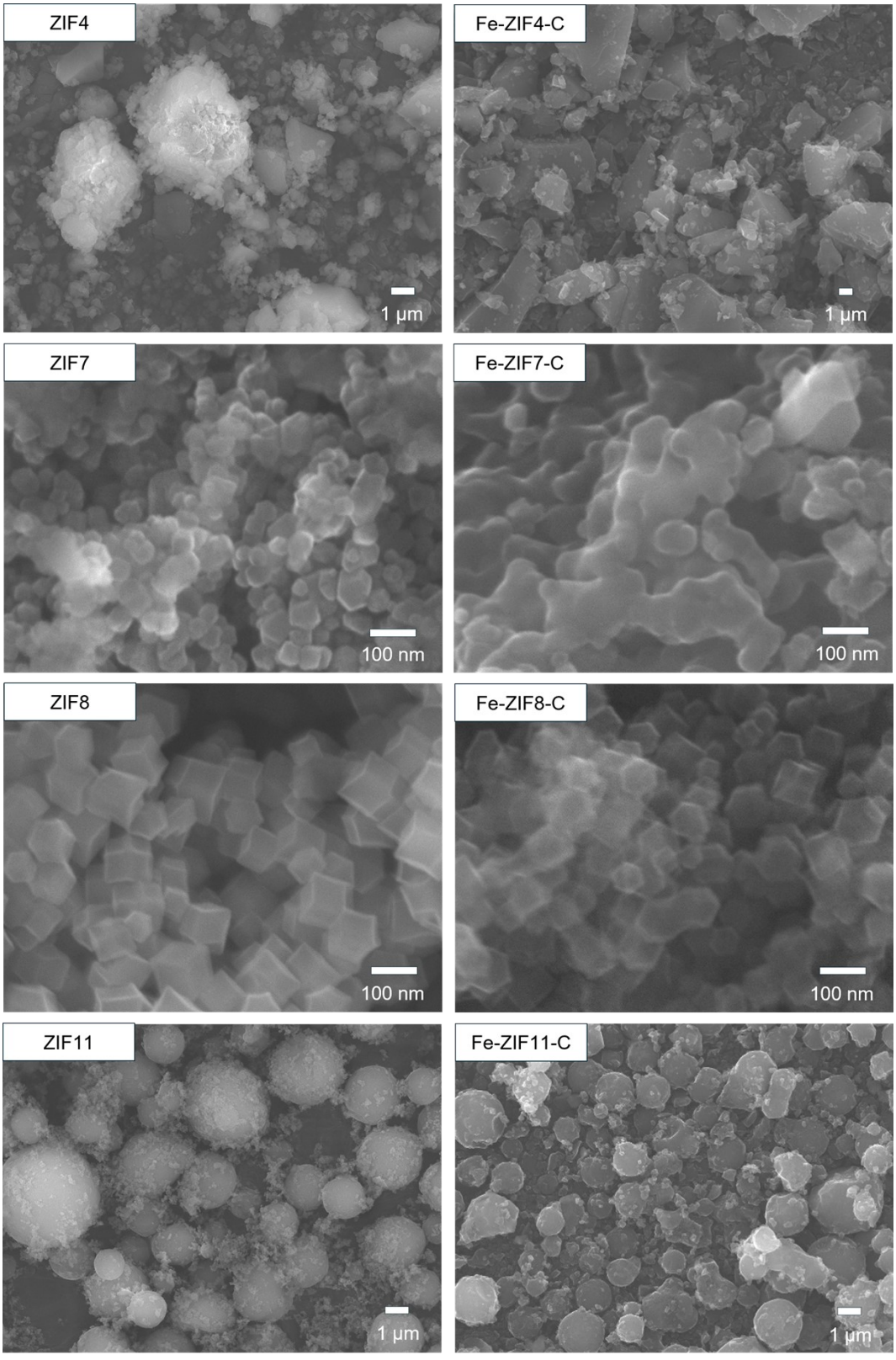

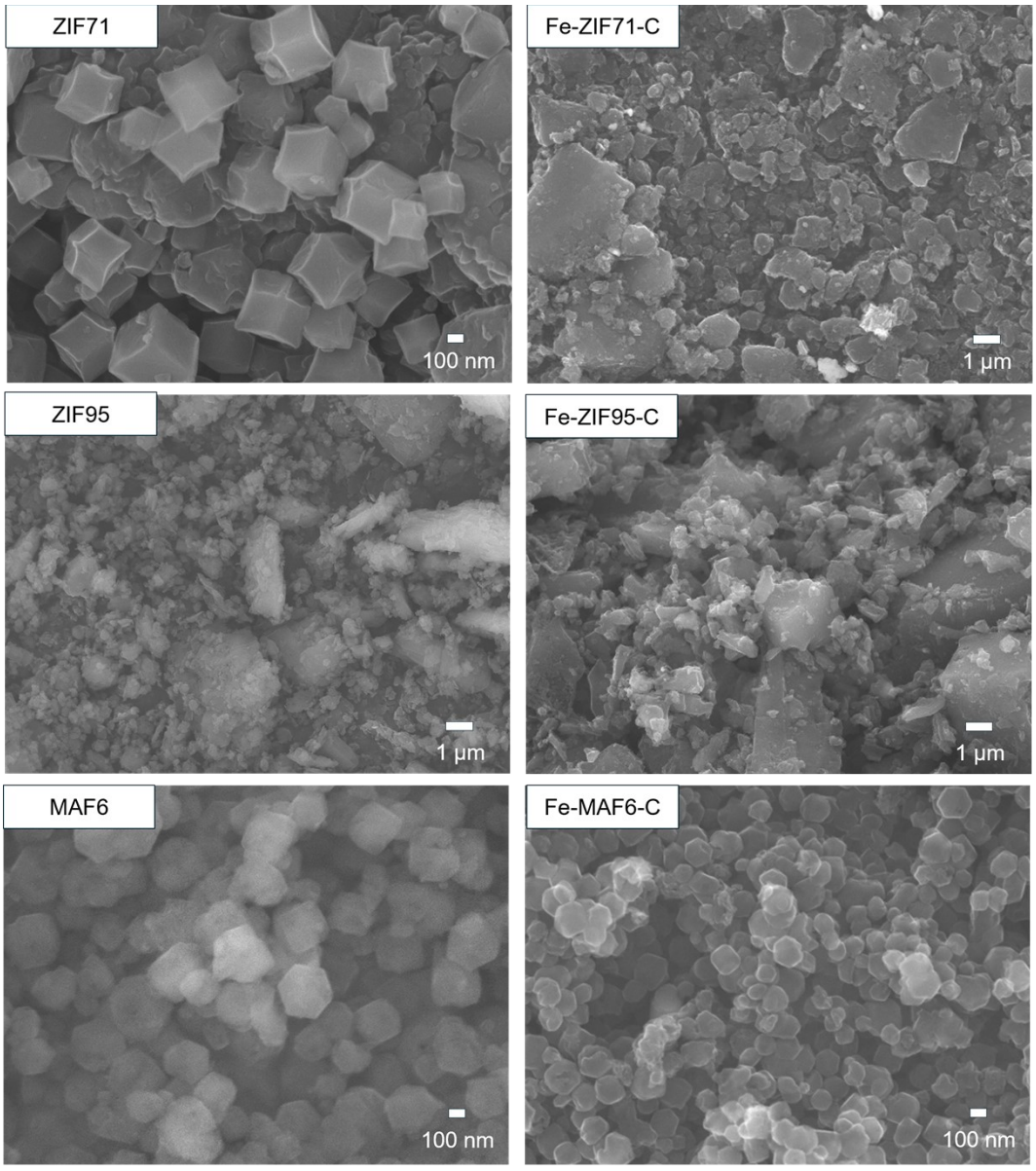

Figure S3. FE-SEM images characterizing synthesized MOFs and the corresponding carbonized samples.

S9. Ar physisorption and pore size analysis of MOF-derived carbons

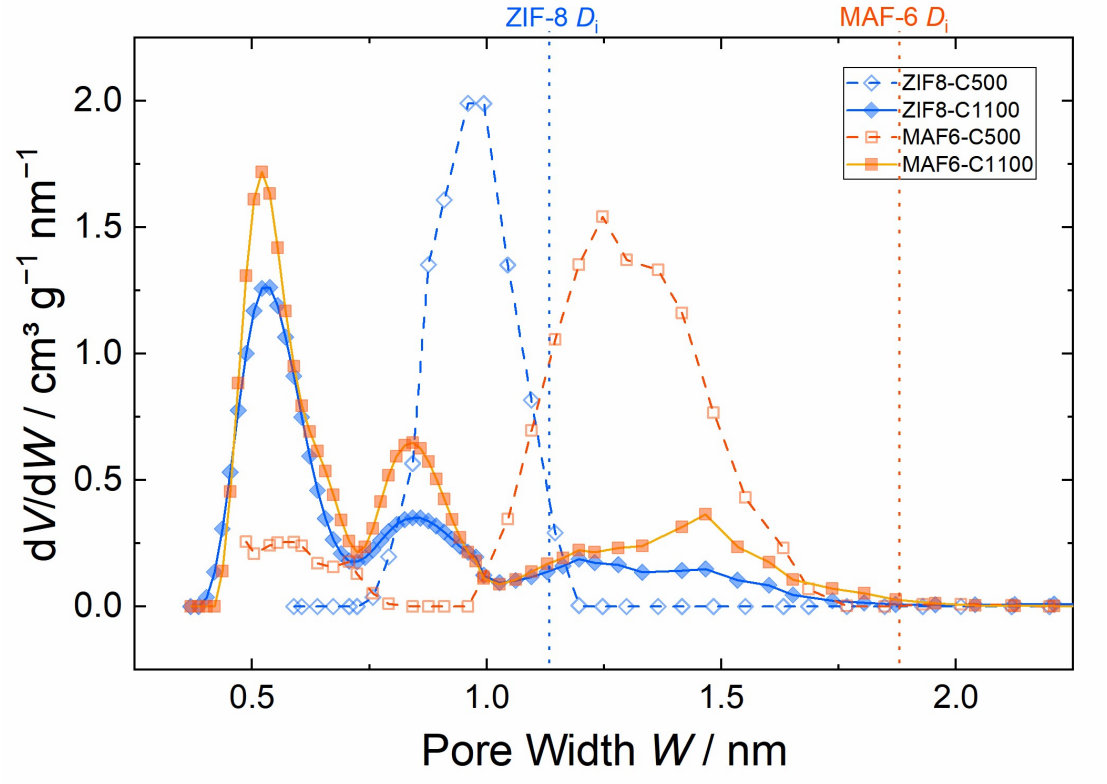

Figure S4. Pore-size distributions of ZIF-8 and MAF-6-deriveds samples pyrolyzed at 500 or 1100 ºC.

S10. Correlation of microporosity with structural descriptors of MOFs

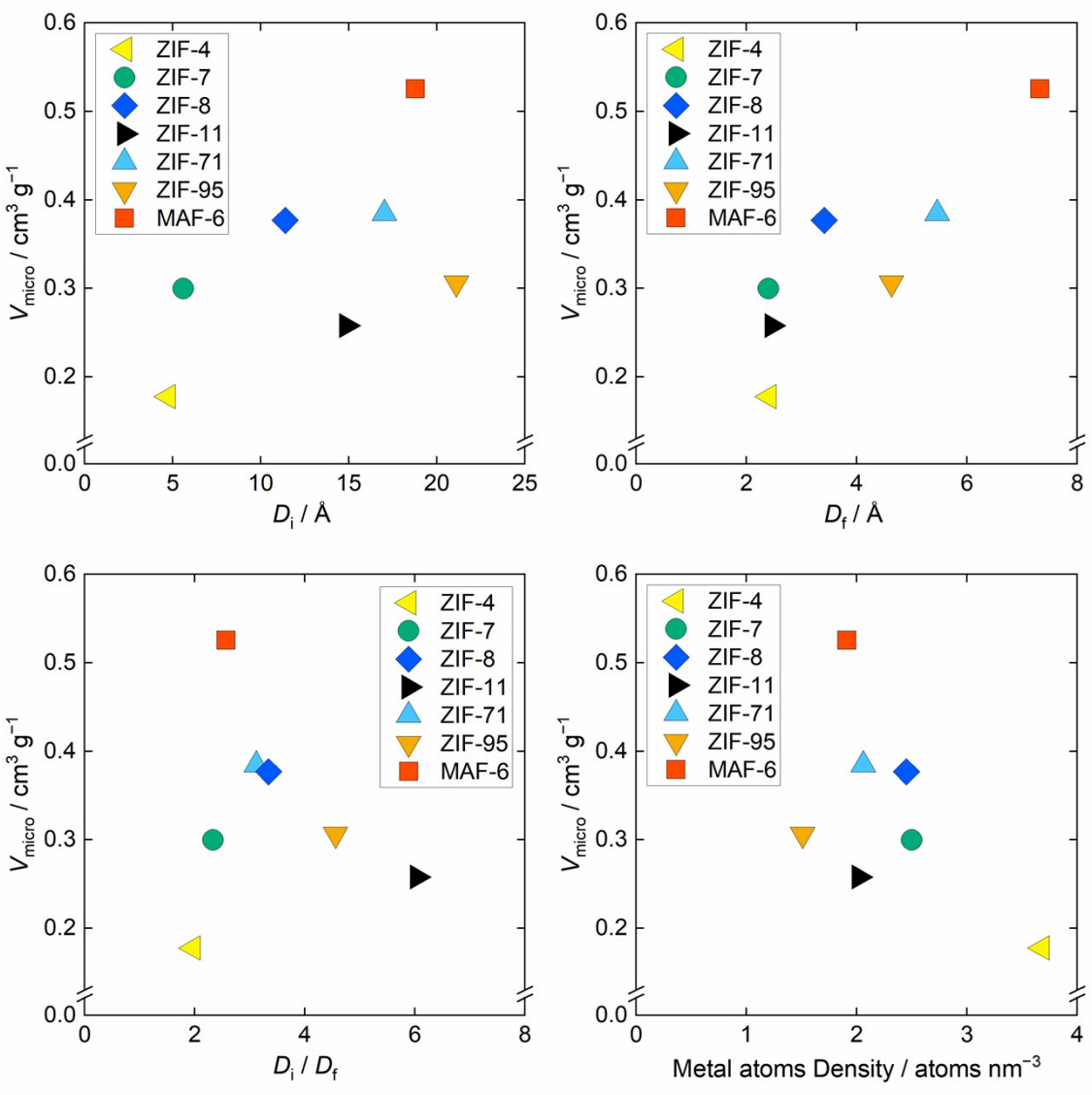

Figure S5. Total micropore volume (V_{micro}) of MOF-derived carbons plotted against D_i (top left), D_f (top right), D_i/D_f ratio (lower left), and metal atom density (lower right).

S11. Comparison of Ar and N_2 physisorption data

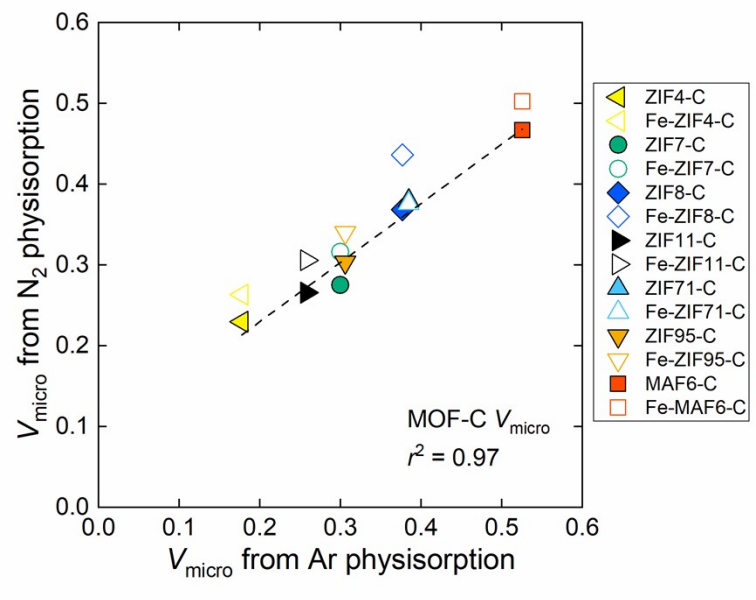

Figure S6. Comparison of micropore volume (V_{micro}) obtained from high-resolution Ar physisorption with 2D-NLDFT-HS and from N_2 physisorption analyzed using the method in Section S1-4 for MOF-derived carbons. The strong linear correlation confirms the consistency between the two measurement approaches despite differences in probe molecules and analysis methods.

S12. Electrochemical quantification of Fe–N_x site density (SD)

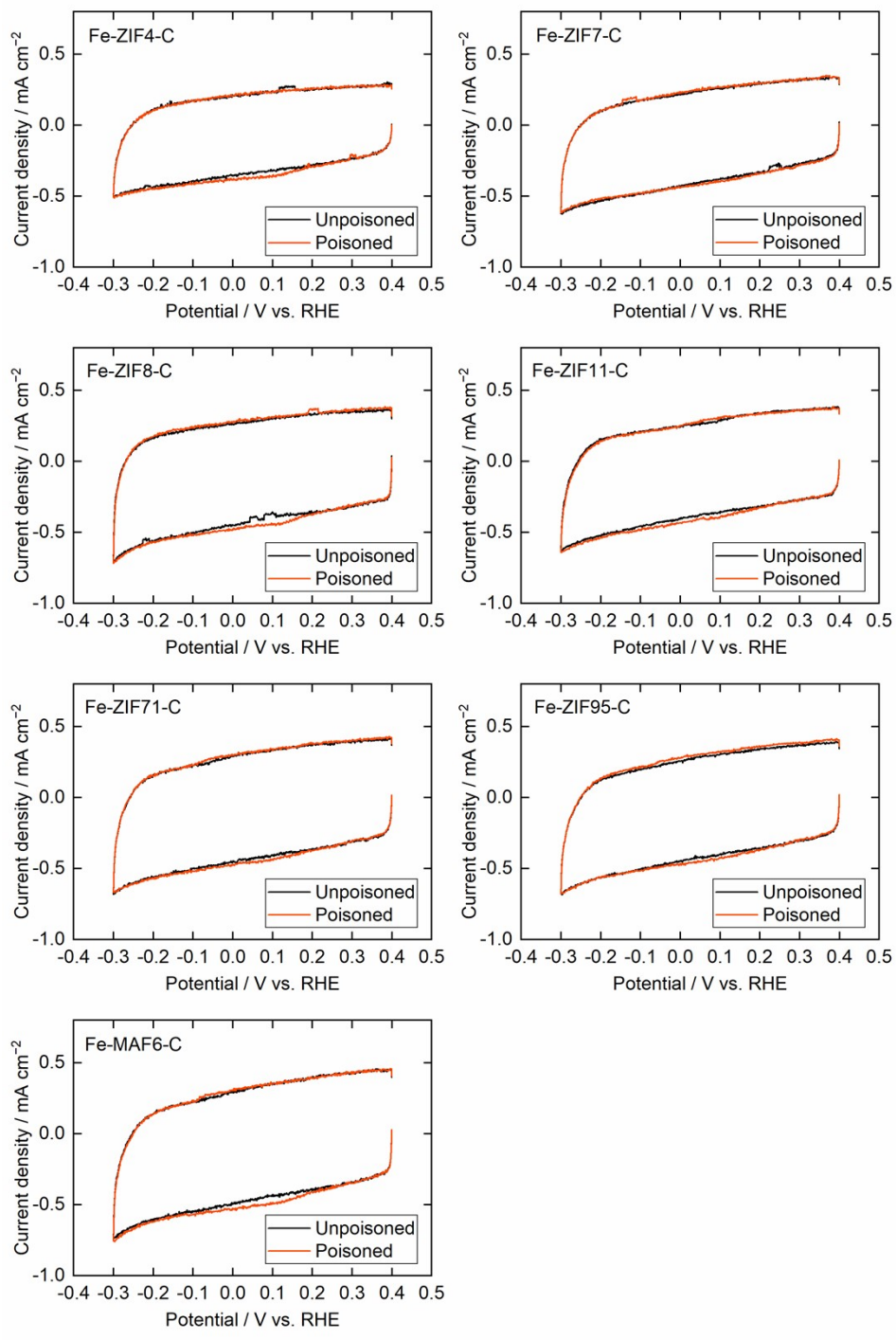

Figure S7. Cyclic voltammograms recorded in N_2-saturated 0.5 M acetate buffer (pH 5.2) at 10 mV s^{-1} before (black) and after (red) NO poisoning for Fe–N–C catalysts.

S13. Correlation of Fe–N_x site density with microporosity and nitrogen content

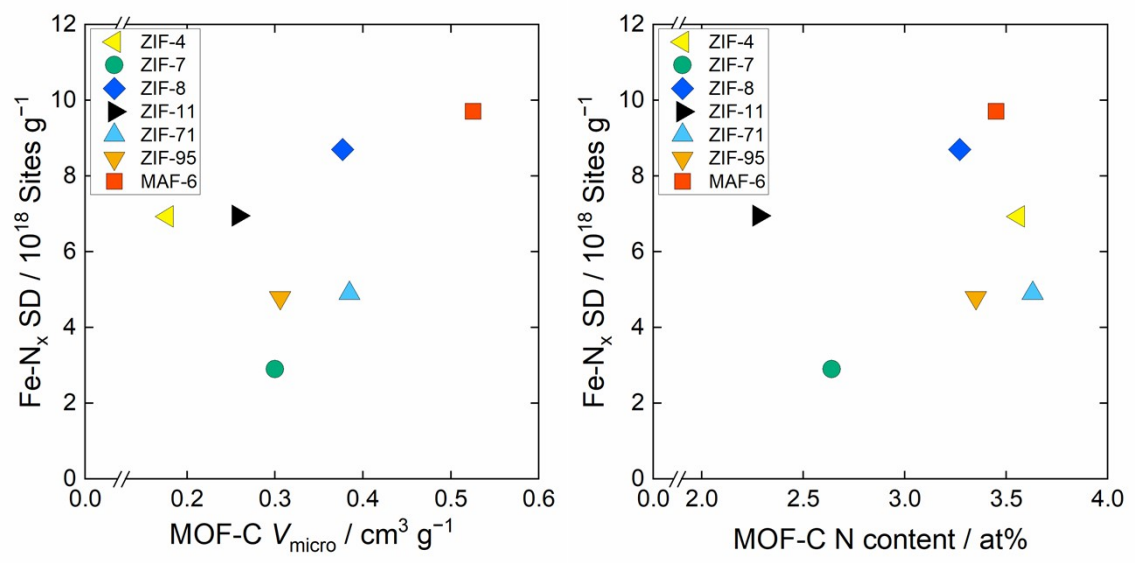

Figure S8. Relationship between Fe–N_x site density (SD), quantified by electrochemical reductive stripping of NO, and (left) the total micropore volume (V_{micro}) of MOF-derived carbons (MOF-C) and (right) the total nitrogen content of MOF-C determined by XPS.

S14. Linear sweep voltammetry of ORR for Fe–N–C catalysts

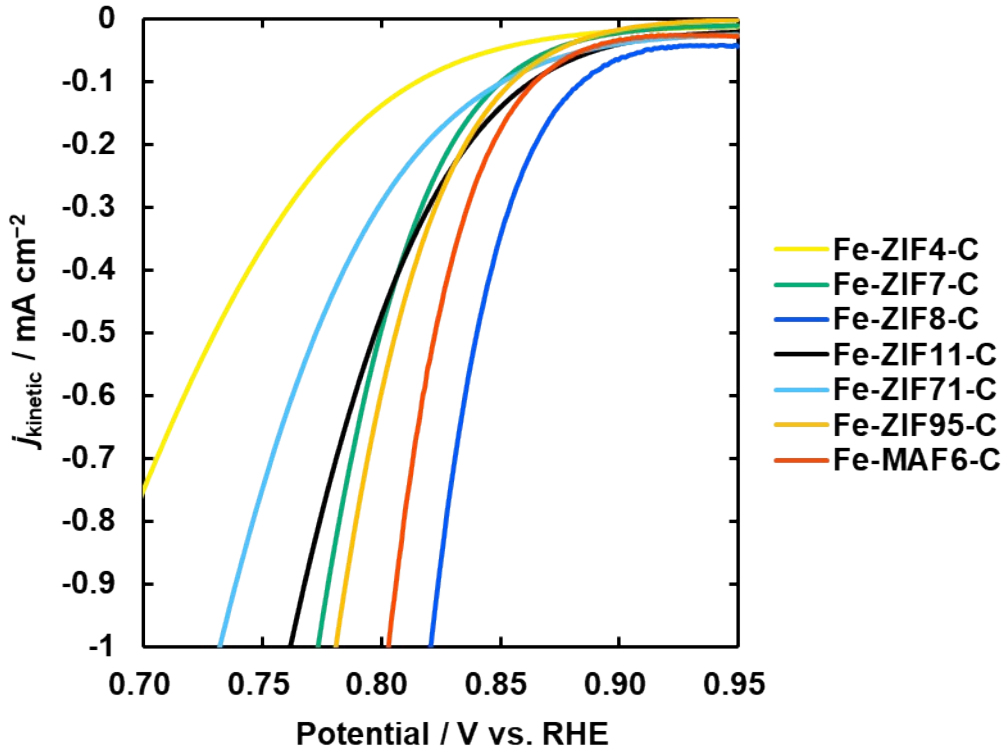

Figure S9. Linear sweep voltammetry curves of Fe–N–C catalysts derived from different MOF precursors, measured in O_2-saturated 0.5 M H_2SO_4 electrolyte at 25 ºC using a three-electrode cell equipped with a rotating disk electrode (RDE). Measurements were performed at a catalyst loading of 800 μg cm^{-2} and a rotation speed of 1,700 rpm.

S15. Site-normalized activity (TOF) of Fe–N–C catalysts

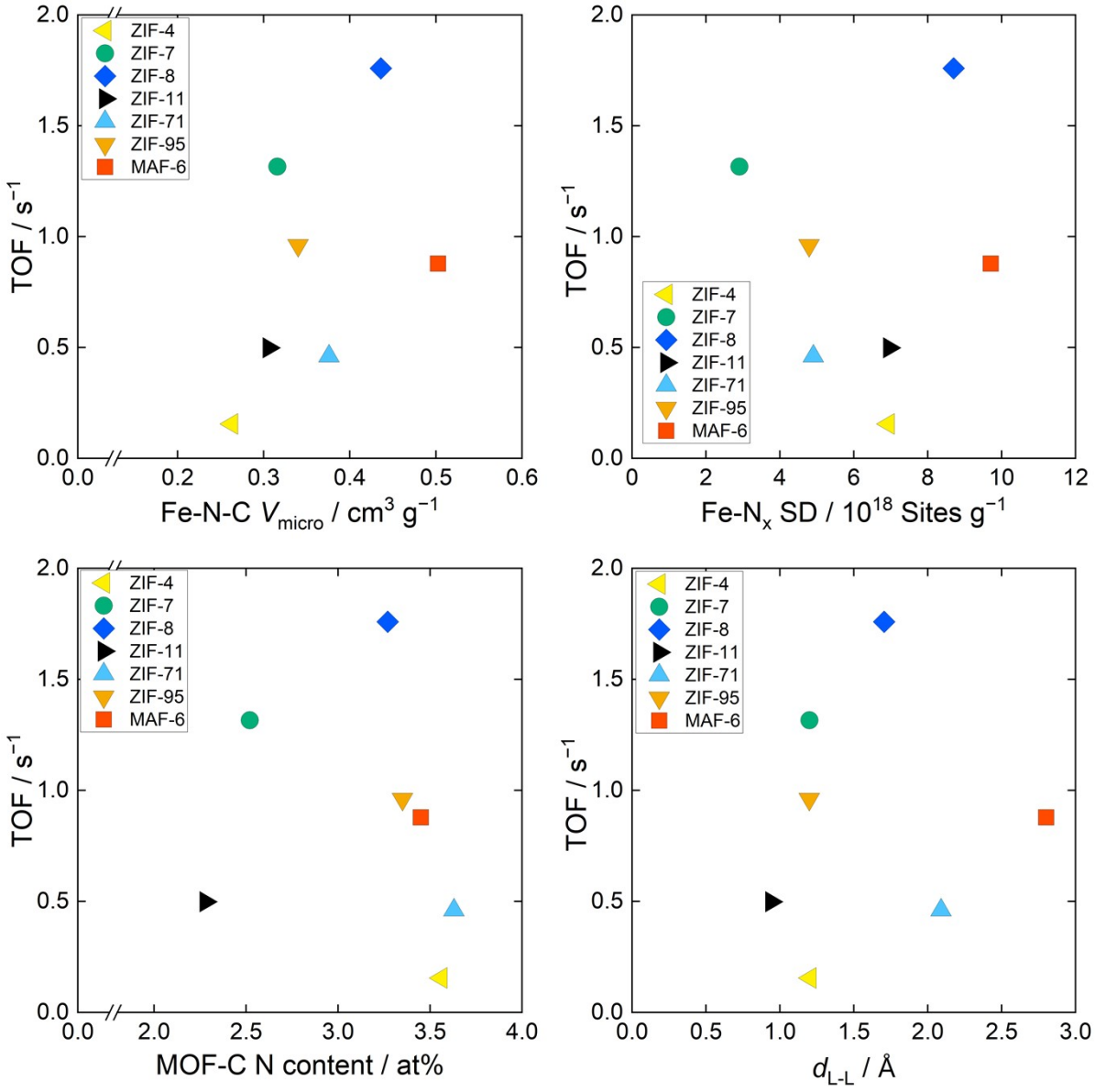

Figure S10. Turnover frequency of Fe–N–C catalysts plotted against V_{micro} (top left), Fe-N_x SD (top right), nitrogen content of MOF-derived carbons (lower left) and d_{L-L} of the parent MOFs (lower right).

References

[1] J. Zhang, A. Qiao, H. Tao, Y. Yue, *J. Non-Cryst. Solids* **2019**, *525*, 119665.

[2] F. Şahin, B. Topuz, H. Kalıpçılar, *Microporous Mesoporous Mater.* **2018**, *261*, 259–267.

[3] H. Zhang, S. Hwang, M. Wang, Z. Feng, S. Karakalos, L. Luo, Z. Qiao, X. Xie, C. Wang, D. Su, Y. Shao, G. Wu, *J. Am. Chem. Soc.* **2017**, *139*, 14143–14149.

[4] M. He, J. Yao, Q. Liu, Z. Zhong, H. Wang, *Dalton Trans.* **2013**, *42*, 16608–16613.

[5] R. P. Lively, M. E. Dose, J. A. Thompson, B. A. McCool, R. R. Chance, W. J. Koros, *Chem. Commun.* **2011**, *47*, 8667–8669.

[6] X. Ma, Y. Li, A. Huang, *J. Membr. Sci.* **2020**, *597*, 117629.

[7] M. N. Timofeeva, I. A. Lukoyanov, V. N. Panchenko, B. N. Bhadra, E. Y. Gerasimov, S. H. Jhung, *Catalysts* **2021**, *11*.

[8] J. Li, H. Zhang, W. Samarakoon, W. Shan, D. A. Cullen, S. Karakalos, M. Chen, D. Gu, K. L. More, G. Wang, Z. Feng, Z. Wang, G. Wu, *Angew. Chem. Int. Ed.* **2019**, *58*, 18971–18980.